doi: 10.18720/MCE.82.16

Finite element models in stresses for bending plates

Конечно элементные модели в напряжениях для изгибаемых пластин

Yu.Ya. Tyukalov,
Vyatka State University, Kirov, Russia

Д-р техн. наук, профессор Ю.Я. Тюкалов,
Вятский государственный университет, г. Киров, Россия

Key words: finite element method; moments approximation; bending plates; buildings; constructions

Ключевые слова: метод конечных элементов; аппроксимация моментов; изгибаемые пластины; здания; конструкции

Abstract. Finite element models for plate bending problems are constructed on the basis of approximations of moments fields. The bending and twisting moments are approximated in the finite element area by piecewise constant functions. The solution is based on the functional of the additional energy. Algebraic equations of equilibrium of nodes of grid of finite elements are formed using the principle of possible displacements and are included in the functional with the help of Lagrange multipliers. The necessary expressions for rectangular and triangular finite elements are obtained. Calculations of square clamped and hinged-supported plates on the action of uniformly distributed load are performed. Comparison of the obtained results with the results by the finite element method calculations in displacements is presented. It is shown that the presented method of calculating bent plates by the finite element method in stresses has the property of convergence from above. The displacements obtained by this method converge to the exact values from above, while the values of the moments is determined with reserve. When the grid of finite elements is crushed, the difference of the two solutions, in stresses and in displacements, decreases monotonically and the accuracy of the obtained results can be estimated from the value of this difference.

Аннотация. Конечно-элементные модели для задач изгиба пластин построены на основе аппроксимаций полей моментов. Изгибающие и крутящие моменты аппроксимируются по области конечных элементов кусочно-постоянными функциями. Решение строится на основе функционала дополнительной энергии. Алгебраические уравнения равновесия узлов сетки конечных элементов формируются при помощи принципа возможных перемещений и включаются в функционал при помощи множителей Лагранжа. Получены необходимые выражения для прямоугольных и треугольных конечных элементов. Выполнены расчеты квадратных защемленных и шарнирно-опертых плит на действие равномерно распределенной нагрузки. Приведено сравнение полученных результатов с результатами расчетов по методу конечных элементов в перемещениях. Показано, что представленный метод расчета изгибаемых пластин методом конечных элементов в напряжениях обладает свойством сходимости сверху – перемещения, полученные данным методом сходятся к точным значениям сверху, при этом величины моментов определяются в запас прочности. При измельчении сетки конечных элементов разность двух решений, в напряжениях и в перемещениях, монотонно уменьшается и по величине этой разности можно оценивать точность полученных результатов.

1. Introduction

Bending plates are widely used in construction of various buildings and structures. They are important constructive elements. From their strength very often depends the security and reliability of the entire structure. A more accurate definition of the internal forces, arising in bent plates, from various types of loads and impacts, remains an actual task now. Therefore, a lot of scientific articles and books are devoted to the construction of various finite elements modeling the bending of plates [1, 2], but the problem remains topical.

When finite element method is used based on the displacements fields approximation, it is difficult to select suitable functions for the approximations [3–6]. As is known, when we solve problems of bending of plates by the finite element method, the polynomials, used to approximate the displacements, must have higher order, in comparison with the plane problem of the theory of elasticity. It is difficult to ensure the continuity of the stress fields at the node points and along the boundaries of the finite elements [2]. Stresses

Тюкалов Ю.Ю. Конечно элементные модели в напряжениях для изгибаемых пластин // Инженерно-строительный журнал. 2018. № 6(82). С. 170–190.

and forces are usually determined for the central points of finite elements. In [7, 8], displacement fields along the boundaries of finite elements are accorded by means of additional equations introduced by means of penalty functions or Lagrange multipliers.

In paper [9], the Ritz method is used to solve the problem of nonlinear bending of elliptic plates, and comparison is made with the solutions of other authors. The construction of finite elements for bent plates is possible based on the application of the equations of the three-dimensional theory of elasticity [10, 11]. This approach allows to obtain good results when analyzing thick plates, when it is necessary to consider the shear strains.

A few papers are devoted to the use of mixed and hybrid methods for the construction of finite elements [12–15]. With this approach, the approximations of displacement fields and stress (force) fields are used, which leads to an increase in the total number of unknowns. In addition, the obtained solutions do not possess the properties of the lower or upper boundary. In [16], the displacement function is chosen as polynomial of the fourth degree to solve the problem of bending of clamped rectangular plate. The results of calculations of deflections, bending moments and shearing forces for square plates of different thicknesses are presented and compared with the results of other authors.

The finite element models for bending the plate according to the Kirchhoff theory can be constructed since approximations only for forces [17–19]. In this case, the solution is built on the basis functional of the additional energy. Algebraic equilibrium equations for nodes are forming using the principle of possible displacements and they are including in the functional as penalty functions. It is shown that in the case of using piecewise-constant functions to approximate the nodal moments, the solution has property of upper boundary.

In [22], a comparative analysis of different types of finite elements is carried out for the calculation of bent plates. More than ten types of finite elements are developed since the Lagrange principle, and they have a different number of degrees of freedom in the form of nodal displacements and angles of rotation. Also presented many finite elements developed since mixed variational principles, when both nodal forces and displacements are used as unknowns. In book consider only two finite elements developed since the method of forces having 9 and 16 degrees of freedom. Obviously, finite elements based on the method of forces are not developed enough.

To solve the plates bending problems, incompatible elements of the displacement method building based on the Lagrange functional are widely used. When formulating such elements, additional conditions are introduced for matching the slope angles of the normal along the boundaries of finite elements [24, 25], or independent approximations are used for displacements and angles of rotation [26, 27, 30], and then additional conditions are used to harmonize the introduced approximations. Also, various hybrid [27, 28], equilibrium [33] and mixed formulations [35] of the finite element method are used for the solution.

The present paper is aimed at constructing the solution of the problem of bending of Kirchhoff plates by the finite element method based on approximation of forces and using only the principles of minimum of additional energy and possible displacements.

2. Methods

The solution of plate bending problems in stresses can be obtained using the additional energy functional [1, 2]:

$$\Pi^c = U^* + V^* = \frac{1}{2}\int \{M\}^T [E]^{-1}\{M\} d\,\Omega - \int \{T\}^T \{\overline{\Delta}\} dS \to min, \quad (1)$$

U^* – additional energy of the strains, V^*– potential of boundary forces corresponding to the specified displacements [1]; $\{\overline{\Delta}\}$ – vector given displacements of nodes; $\{T\}$ – vector boundary forces; S – boundary surface, on which the displacement nodes are given; Ω – subject area; $\{M\} = \begin{Bmatrix} M_x \\ M_y \\ M_{xy} \end{Bmatrix}$ – vector of bending and torsional moments; $[E]^{-1}$ – matrix of flexibility of the material:

$$[E]^{-1} = \frac{12}{E \cdot t^3}\begin{bmatrix} 1 & -\mu & 0 \\ -\mu & 1 & 0 \\ 0 & 0 & 2(1+\mu) \end{bmatrix}, \quad (2)$$

where: E – modulus of elasticity of the material; μ is the Poisson ratio; t is the thickness of the plate.

In accordance with the principle of minimum additional energy, the moments functions M_x, M_y, M_{xy}, must satisfy the differential equations of equilibrium. The system of differential equations of equilibrium for bent plates, under the action of distributed load q, has the following form [2]:

$$\begin{cases} \dfrac{\partial Q_x}{\partial x} + \dfrac{\partial Q_y}{\partial y} + q = 0, \\ \dfrac{\partial M_x}{\partial x} + \dfrac{\partial M_{xy}}{\partial y} - Q_x = 0, \\ \dfrac{\partial M_y}{\partial y} + \dfrac{\partial M_{xy}}{\partial x} - Q_y = 0. \end{cases} \quad (3)$$

Eliminating the transverse forces Q_x and Q_y from (3), we obtain the known differential equation of equilibrium of second-order:

$$\frac{\partial^2 M_x}{\partial x^2} + 2\frac{\partial^2 M_{xy}}{\partial x \partial y} + \frac{\partial^2 M_y}{\partial y^2} + q = 0. \quad (4)$$

Since, in the general case, it is practically impossible to select the basis functions for M_x, M_y, M_{xy}, which satisfy the differential equation (4), it is suggested to introduce additional stress functions of Southwell [2]. Then the moments are expressed in terms of the derivatives of the introduced stress functions. This approach leads to additional difficulties in specifying loads and boundary conditions and has not received wide practical spread.

In [17–19] another approach is proposed for the solution. The subject area is divided into rectangular or triangular finite elements. The fields of moments in the region of the finite element can be approximated by linear or piecewise constant functions (Figure 1). Linear approximating functions (Figure 1a) ensure the continuity of the moment fields across the entire subject area. Piecewise-constant functions (Figure 1b) satisfy the differential equation of equilibrium (4) in the absence of a distributed load and are continuous along the boundaries of finite elements but have discontinuities inside the region of the finite element.

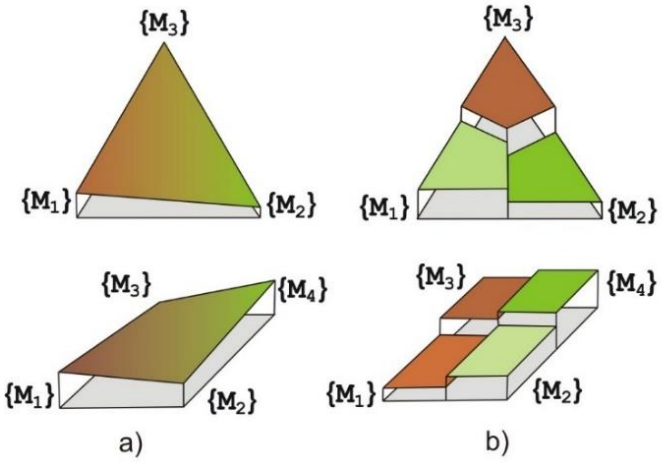

Figure 1. Variants of the approximation of moments in the region of the finite element: a) the moments vary linearly; b) the moments are piecewise-constant

For simplicity, we assume that the given node displacements are absent. Then, using for moments any variant of approximating functions (Figure 1), the expression for the functional (1) can be written in the following matrix form:

$$\Pi^c = \frac{1}{2}\{M\}^T [D]\{M\} \to min, \quad (5)$$

where $\{M\}$ is a vector of unknown stresses for the whole system; $[D]$ is the matrix of flexibility for the entire system.

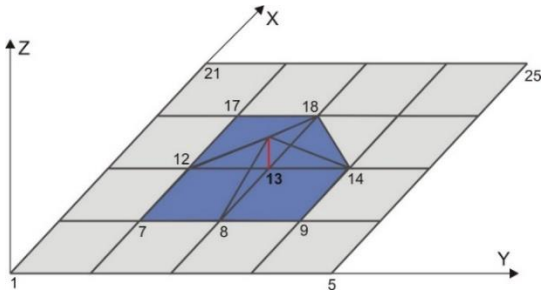

Figure 2. Possible displacement of the node 13 and adjacent finite elements

Using the principle of possible displacements (Figure 2), for all non-supported nodes of the system, we will get algebraic equations of equilibrium of forces along the vertical axis Z:

$$\{C_i\}^T\{M_i\} + \overline{P}_i = 0, i \in \Xi_z. \tag{6}$$

where$\{M_i\}$ is the vector of unknown node moments of all finite elements adjacent to node i; Ξ_z is the set of nodes, that have non-fixed displacement along the vertical axis Z; $\overline{P}_i$ is the generalized force corresponding to the potential of external loads for possible displacements of node i along the Z axis; $\{C_i\}$ is vector containing coefficients on unknown node moments in the equilibrium equation of node i along the Z axis. Algebraic equilibrium equations (6) ensure the equilibrium of the moment fields in discrete sense. Unknown parameters are only the moments in nodes of finite elements grid. In [17–19], the solution of this problem was considered using the penalty functions method, which makes it possible to obtain the functional (7):

$$\Pi^c = \frac{1}{2}\{M\}^T[D]\{M\} + \sum_{i\in\Xi_z} \propto \left(\{C_i\}^T\{M_i\} + \overline{P}_i\right)^2. \tag{7}$$

$\propto$ is the penalty parameter, recommendations for the choice of which are given in [17–19]. Equating the derivatives (7) along the unknown nodal moments to zero, we obtain a system of linear algebraic equations. The matrix of non-zero coefficients of this system of equations will have ribbon structure for any variant of the moments approximation.

In this paper, to minimize the functional (5), in the presence of constraints in the form of system of algebraic equations (6), we will use the method of Lagrange multipliers:

$$\Pi^c = \frac{1}{2}\{M\}^T[D]\{M\} + \sum_{i\in\Xi_z} w_i\left(\{C_i\}^T\{M_i\} + \overline{P}_i\right) \to min, \tag{8}$$

w_i – vertical displacement of node i. In this solution, additional unknowns appear in the form of node displacements. But we must accent that the approximations of the displacement field in region of finite element are not used in the getting (8).

We represent the expression (8) in form more convenient for constructing the solution:

$$\Pi^c = \frac{1}{2}\{M\}^T[D]\{M\} + \{w\}^T(\{F\} - [L]\{M\}) \to min, \tag{9}$$

where $\{w\}$ is the global vector of unknown nodal displacements for the whole system; $\{F\}$ is vector whose elements are equal to the works of external forces on the corresponding unit displacements of the nodes; $[L]$ is the matrix of "equilibrium", whose rows are formed from the corresponding vectors $\{C_i\}$. If we equate the derivatives Π^c c along the vector $\{M\}$ to zero, we obtain the equations of consistency of deformations which expressed in the forces:

$$[D]\{M\} - [L]^T\{w\} = 0. \tag{10}$$

Derivatives Π^c along the vector $\{w\}$ are the system of equations of equilibrium of nodes

$$\{F\} - [L]\{M\} = 0. \tag{11}$$

Combining (10) and (11), we obtain the following system of linear algebraic equations:

$$\begin{bmatrix} [D] & -[L]^T \\ -[L] & [0] \end{bmatrix} \begin{Bmatrix} \{M\} \\ \{w\} \end{Bmatrix} = \begin{Bmatrix} 0 \\ -\{F\} \end{Bmatrix}. \tag{12}$$

Expressing the vector $\{M\}$ from the first matrix equation and substituting it into the second, we obtain

$$[K] = [L][D]^{-1}[L]^T, \quad (13)$$

$$[K]\{w\} = \{F\}, \quad (14)$$

$$\{M\} = [D]^{-1}[L]^T\{w\}. \quad (15)$$

Thus, solving the system of algebraic equations (14), we obtain the values of the node displacements $\{w\}$, and then the vector of moments $\{M\}$ from (15).

If linear functions are used to approximate the moments (Figure 1a), then the matrix $[K]$ will be filled and the solution of the system of linear algebraic equations (14) or the direct solution of the system of equations (12) will require large computational costs. Therefore, below, we will consider variant of the approximation of moments in the region of finite element by piecewise constant functions (Figure 1b). In this case, the matrix $[D]$ is block-diagonal, and the matrix $[K]$ will have ribbon structure of non-zero elements.

Will obtain the necessary expressions for the elements of the matrices $[D]$, $[L]$ and the vector $\{F\}$, which enter (9), when rectangular and triangular finite elements are used to discredit the subject area (Figure 3).

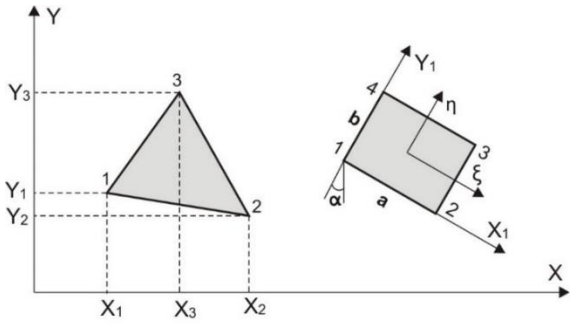

Figure 3. Triangular and rectangular finite elements

We introduce the following notations: $\{\overline{M}_i\} = \begin{Bmatrix} \overline{M}_{i,x} \\ \overline{M}_{i,y} \\ \overline{M}_{i,xy} \end{Bmatrix}$ – vector of moments in node i in local coordinate system X_1OY_1; $\{M_i\} = \begin{Bmatrix} M_{i,x} \\ M_{i,y} \\ M_{i,xy} \end{Bmatrix}$ – vector of moments at node i in the global coordinate system XOY. $M_{i,x}$ – bending moment at node i, directed along the *X* axis; $M_{i,y}$ is the bending moment at node i, directed along the *Y* axis; $M_{i,xy}$ is the torque at node i.

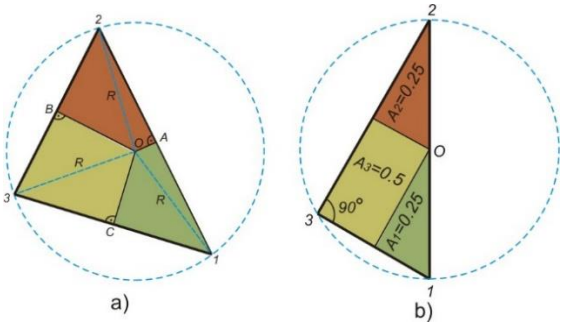

Figure 4. Separation of a triangular finite element into regions with constant moments: a) an arbitrary triangle; b) right-angled triangle

Since the bending moments and torques are piecewise constant, the expression for the additional deformation energy in the global coordinate system can be written in the form of simple sum:

$$U^* = \frac{1}{2}\sum_{i=1}^{m} A_i \{M_i\}^T [E]^{-1} \{M_i\}, \quad (16)$$

$$A_i = \sum_{s=1}^{n_{i,R}} \frac{1}{4} A^s + \sum_{s=1}^{n_{i,T}} A_i^s. \quad (17)$$

where m is the total number of nodes; $n_{i,R}$ is the number of rectangular elements connected to node i; $n_{i,T}$ – the number of triangular elements connected to node i; A^s is the area of finite element. We introduce the notation for the flexibility matrix of "neighborhoods" of the node i; A_i^s is the area of the part of the triangular finite element with constant bending moments (Figure 4a). This point can be defined as the point of intersection of perpendiculars, drawn from the middle of the sides (Figure 4a).

For a rectangular finite element, the separation of an element into regions with constant moments is uniquely – into four equal regions. For a triangular element, each side must be equally divided, but there must also be a point inside the element in which the three areas, related to the nodes, intersect. If the largest angle of the triangle is greater than 90 degrees, then such a point lies outside the triangle. In this case, the triangle is divided into regions by lines passing through the middle of the sides – these lines will be parallel to the sides of the triangle. Such a division of a triangular element into regions with constant moments makes it possible to obtain more accurate results, than in the case of division simply into three equal parts – $\frac{1}{3}A^s$.

In Figure 4a, the point O is the center of a circle described about the triangle. OA, OB, OC – perpendiculars, directed from the middle of the corresponding sides of the triangle. Denote the lengths of the sides of the triangle – l_{12}, l_{23}, l_{31}. From the schemes in Figure 4a we get:

$$R = \frac{l_{12} l_{23} l_{31}}{4A^s},$$

$$A_1^s = \frac{l_{12}}{4}\sqrt{R^2 - \frac{{l_{12}}^2}{4}} + \frac{l_{31}}{4}\sqrt{R^2 - \frac{{l_{31}}^2}{4}},$$

$$A_2^s = \frac{l_{12}}{4}\sqrt{R^2 - \frac{{l_{12}}^2}{4}} + \frac{l_{23}}{4}\sqrt{R^2 - \frac{{l_{23}}^2}{4}}, \quad (18)$$

$$A_3^s = \frac{l_{23}}{4}\sqrt{R^2 - \frac{{l_{23}}^2}{4}} + \frac{l_{31}}{4}\sqrt{R^2 - \frac{{l_{31}}^2}{4}}.$$

It is obvious that for a right-angled triangle (Figure 4b) – $A_1^s = A_2^s = \frac{1}{4}A^s, A_3^s = \frac{1}{2}A^s$. For an equilateral triangle – $A_1^s = A_2^s = A_3^s = \frac{1}{3}A^s$. If one of the angles of triangle is greater than $90°$, then, as well as for a right-angled triangle, we take: $A_1^s = A_2^s = \frac{1}{4}A^s, A_3^s = \frac{1}{2}A^s$. Besides, you do not need to use too elongated triangles. Better such triangles divided into two more correct triangles.

We introduce the notation for the flexibility matrix of "neighborhoods" of node i and for the global flexibility matrix for the entire system, which consists of matrices of flexibility for all nodes of the system:

$$[D_i] = A_i [E]^{-1}, [D] = \begin{bmatrix} [D_1] & & \\ & \ddots & \\ & & [D_m] \end{bmatrix}. \quad (19)$$

It is obvious that the matrix $[D]$ is easily invertible analytically.

$$[D]^{-1} = \begin{bmatrix} [D_1]^{-1} & & \\ & \ddots & \\ & & [D_m]^{-1} \end{bmatrix}. \quad (20)$$

Consider the derivation of the equilibrium equations for possible displacement of node of rectangular finite element in the local coordinate system $X_1 O Y_1$ (Figure 5). For rectangular finite element, we introduce also the local coordinate system $\xi c \eta$, connected with its center (Figure 5) and enter the basic functions, which are expressed in normalized local coordinates in the following form:

$$N_i(x,y) = \frac{(1+\xi_i\xi)(1+\eta_i\eta)}{4}, \xi = \frac{2x}{a}, \eta = \frac{2y}{b}, i = 1,2,3,4. \quad (21)$$

The index i denotes the local node number of the finite element; x, y - coordinates along the axes X_1 and Y_1, respectively; ξ_i, η_i are the local normalized coordinates of the node i taking the values 1 or -1. The nodes are numbered counterclockwise, beginning with the lower-left node.

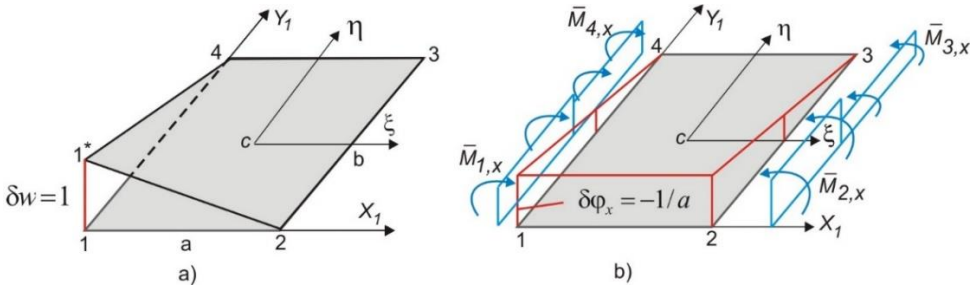

Figure 5. a – possible displacement of the node 1 and deformation of the rectangular finite element; b – the red line shows the graph of the change in the angle of rotation $\delta\varphi_x$ of the sides of the finite element from the possible movement of the node 1

The displacements of the points of the finite element after the possible displacement of the node i ($i = 1,2,3,4$) can be expressed in the following form:

$$\delta w = \frac{(1+\xi_i\xi)(1+\eta_i\eta)}{4}. \quad (22)$$

Possible displacements along each coordinate axis vary linearly, so the curvatures δk_x and δk_y along the axes X_1 and Y_1 are respectively zero, and the torsional curvature δk_{xy} is constant.

$$\delta k_x = -\frac{\partial^2(\delta w)}{\partial x^2} = 0, \delta k_y = -\frac{\partial^2(\delta w)}{\partial y^2} = 0, \delta k_{xy} = -\frac{\partial^2(\delta w)}{\partial x \partial y} = -\frac{2\xi_i\eta_i}{a \cdot b}. \quad (23)$$

Thus, with possible displacement of node i, only internal torques $\overline{M}_{xy}$ and normal bending moments $\overline{M}_n$ along the boundaries of finite elements Γ^e at the corresponding rotation angles $\delta\beta_n$ will work. Then the work of internal forces for the finite element k on possible displacements of node i can be expressed in the following form:

$$\delta U^k_{i,z} = \int_0^a \int_0^b \overline{M}_{xy}\, \delta k_{xy} dxdy + \int_{\Gamma^e} \overline{M}_n\, \delta\beta_n ds. \quad (24)$$

For the boundaries of element directed along the X_1 axis, the bending moment $\overline{M}_y$ and the corresponding angle of rotation of the finite element along the axis Y_1 – $\delta\varphi_y$ are normal. For boundaries directed along the axis Y_1, respectively $\overline{M}_x$ and $\delta\varphi_x$ are normal (Figure 5b).

$$\delta\varphi_x = \frac{\partial(\delta w)}{\partial x} = \frac{\xi_i(1+\eta\eta_i)}{2a}, \delta\varphi_y = \frac{\partial(\delta w)}{\partial y} = \frac{\eta_i(1+\xi\xi_i)}{2b}. \quad (25)$$

In Figure 5b, the red line shows the graph of the change in the angle of rotation along the boundaries of the finite element after possible displacement of the node 1.

Considering that the moments are constant in each quarter of the finite element, the first integral in expression (24) is calculated simply:

$$\int_0^a \int_0^b M_{xy}\, \delta k_{xy} dxdy = \frac{ab}{4} \sum_{j=1}^4 \overline{M}_{xy,j} \delta k_{xy} = -\frac{\xi_i\eta_i}{2} \sum_{j=1}^4 \overline{M}_{xy,j}. \quad (26)$$

The work of the bending moments $\overline{M}_x$ for the angles of rotation of the sides 1-4 and 2-3 of the finite element (Figure 4b) is calculated by integrals

$$\int_{\Gamma^e} \overline{M}_x\, \delta\varphi_x ds = -\frac{b}{2}\overline{M}_{x,1}\xi_1 \int_{-1}^0 \frac{\xi_i(1+\eta\eta_i)}{2a} d\eta - \frac{b}{2}\overline{M}_{x,4}\xi_4 \int_0^1 \frac{\xi_i(1+\eta\eta_i)}{2a} d\eta - \frac{b}{2}\overline{M}_{x,2}\xi_2 \int_{-1}^0 \frac{\xi_i(1+\eta\eta_i)}{2a} d\eta - \frac{b}{2}\overline{M}_{x,3}\xi_3 \int_0^1 \frac{\xi_i(1+\eta\eta_i)}{2a} d\eta. \quad (27)$$

In expression (27), the coefficients $\xi_1 \div \xi_4$, which are to the right of the moments, consider the directions of the moments $\overline{M}_x$ and of the rotation angle $\delta\varphi_x$. On the side 1-4, the moments $\overline{M}_x$ and the rotation $\delta\varphi_x$ are directed equally, so the first two terms in (27) will be positive, since $\xi_1 = \xi_4 = -1$. On the side 2-3, the moments and the rotation are directed in the opposite direction, so the third and fourth terms will be negative, since $\xi_1 = \xi_4 = 1$. Calculating the integrals in (27), we can obtain the following compact expression:

$$\int_{\Gamma^e} \overline{M}_x \, \delta\varphi_x ds = -\frac{b}{4a}\xi_i \sum_{j=1}^{4} \xi_j \left(1 + \frac{\eta_i\eta_j}{2}\right)\overline{M}_{x,j}. \tag{28}$$

Similarly, one can obtain an expression for the operation of the moments $\overline{M}_y$

$$\int_{\Gamma^e} \overline{M}_y \, \delta\varphi_y ds = -\frac{a}{4b}\eta_i \sum_{j=1}^{4} \eta_j \left(1 + \frac{\xi_i\xi_j}{2}\right)\overline{M}_{y,j}. \tag{29}$$

Summing the expressions (26), (28), and (29), we obtain

$$\delta U_{i,z}^k = -\frac{b}{4a}\xi_i \sum_{j=1}^{4} \xi_j \left(1 + \frac{\eta_i\eta_j}{2}\right)\overline{M}_{x,j} - \frac{a}{4b}\eta_i \sum_{j=1}^{4} \eta_j \left(1 + \frac{\xi_i\xi_j}{2}\right)\overline{M}_{y,j} - \frac{\xi_i\eta_i}{2}\sum_{j=1}^{4} \overline{M}_{xy,j}. \tag{30}$$

Substituting i to be equal from 1 to 4 in (30), we obtain expressions for the operation of internal forces (moments) for possible displacements of nodes from the first to the fourth.

We unite the node moments in the local coordinate system X_1OY_1 for the finite element k to the vector $\left\{\overline{M}^k\right\}$.

$$\left\{\overline{M}^k\right\}^T = \left(\overline{M}_{x,1} \quad \overline{M}_{y,1} \quad \overline{M}_{xy,1} \quad \overline{M}_{x,2} \quad \overline{M}_{y,2} \quad \overline{M}_{xy,2} \quad \overline{M}_{x,3} \quad \overline{M}_{y,3} \quad \overline{M}_{xy,3} \quad \overline{M}_{x,4} \quad \overline{M}_{y,4} \quad \overline{M}_{xy,4}\right). \tag{31}$$

We also introduce vector combining the values of the work of internal forces for possible displacements of nodes of finite element

$$\left\{\delta U_z^k\right\} = \begin{Bmatrix} \delta U_{1,z}^k \\ \delta U_{2,z}^k \\ \delta U_{3,z}^k \\ \delta U_{4,z}^k \end{Bmatrix}. \tag{32}$$

Then we can write the following expression in matrix form:

$$\{\delta U_z^k\} = \left[\overline{L}^k\right]\left\{\overline{M}^k\right\}. \tag{33}$$

Using (30), we obtain expressions for the elements of the matrix $\left[\overline{L}^k\right]$.

$$\left[\overline{L}^k\right] = \begin{bmatrix} \frac{-3b}{8a} & \frac{-3a}{8b} & \frac{1}{2} & \frac{3b}{8a} & \frac{-a}{8b} & \frac{1}{2} & \frac{b}{8a} & \frac{a}{8b} & \frac{1}{2} & \frac{-b}{8a} & \frac{3a}{8b} & \frac{1}{2} \\ \frac{3b}{8a} & \frac{-a}{8b} & \frac{-1}{2} & \frac{-3b}{8a} & \frac{-3a}{8b} & \frac{-1}{2} & \frac{-b}{8a} & \frac{3a}{8b} & \frac{-1}{2} & \frac{b}{8a} & \frac{a}{8b} & \frac{-1}{2} \\ \frac{b}{8a} & \frac{a}{8b} & \frac{1}{2} & \frac{-b}{8a} & \frac{3a}{8b} & \frac{1}{2} & \frac{-3b}{8a} & \frac{-3a}{8b} & \frac{1}{2} & \frac{3b}{8a} & \frac{-a}{8b} & \frac{1}{2} \\ \frac{-b}{8a} & \frac{3a}{8b} & \frac{-1}{2} & \frac{b}{8a} & \frac{a}{8b} & \frac{-1}{2} & \frac{3b}{8a} & \frac{-a}{8b} & \frac{-1}{2} & \frac{-3b}{8a} & \frac{-3a}{8b} & \frac{-1}{2} \end{bmatrix}. \tag{34}$$

The node moments $\left\{\overline{M}^k\right\}$ in local and $\{M^k\}$ in global coordinate system are connected by the matrix of the direction cosines

$$[l] = \begin{bmatrix} \cos^2 \propto & \sin^2 \propto & -2\sin \propto \cos \propto \\ \sin^2 \propto & \cos^2 \propto & 2\sin \propto \cos \propto \\ \sin \propto \cos \propto & -\sin \propto \cos \propto & \cos^2 \propto - \sin^2 \propto \end{bmatrix}. \tag{35}$$

$\propto$ is the angle between the Y_1 axis and the Y axis (Figure 3). Using (35), we obtain the matrix of the direction cosines for the finite element

$$[S^k] = \begin{bmatrix} [l] & & & \\ & [l] & & \\ & & [l] & \\ & & & [l] \end{bmatrix}. \quad (36)$$

The work of internal forces (33) can be represented in the following form:

$$\{\delta U_z^k\} = [L^k]\{M^k\}, [L^k] = \left[\overline{L}^k\right][S^k]. \quad (37)$$

The matrix can be called the local matrix of "equilibrium" of the finite element. From matrices $[L^k]$ for finite elements, in accordance with the numbering of the nodes and elements, global "equilibrium" matrix $[L]$ is formed for the whole system.

The potential of the external concentrated and uniformly distributed loads for possible displacements of the node i along the global coordinate axis is determined by the formula (38).

$$\delta V_i = P_i + \frac{1}{4} q^k ab = R_i. \quad (38)$$

P_i – the force concentrated at node i; q^k – uniformly distributed by element load. The generalized forces R_i are placed in the vector $\{F\}$ (see (12)).

Consider possible displacement of node of triangular finite element (Figure 6). We can express possible displacements of the nodes of finite element using triangular coordinates:

$$\delta w_i(x, y) = L_i, i = 1,2,3. \quad (39)$$

$$L_i = \frac{1}{A}(a_i + b_i x + c_i y), a_i = x_{i+1} y_{i+2} - x_{i+2} y_{i+1}, \quad (40)$$
$$b_i = y_{i+1} - y_{i+2}, c_i = x_{i+2} - x_{i+1}.$$

A is the area of the triangular element; x_i, y_i are the coordinates of node i (Figure 3).

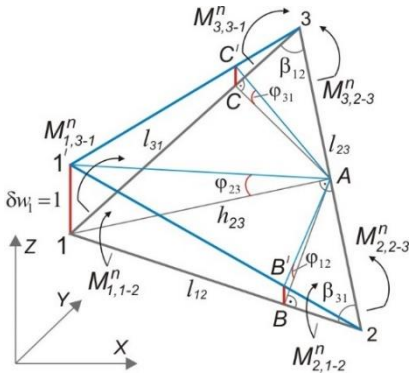

Figure 6. Possible displacement δw_1 of the node 1 of the triangular finite element

Triangular coordinates are the natural coordinates of the triangular region. The function L_i takes value of 1 in node i and values of zero in the other two nodes. Since the function L_i is linear with respect to x and y coordinates, curvatures δk_x and δk_y along the X and Y axes, respectively, and torsional curvature δk_{xy} for a possible node displacement will be zero. In this case, the finite element moves as rigid whole without deforming, and the work will be performed only by bending moments M^n normal to boundaries of the finite element on the corresponding angles of rotation of the sides of the element (Figure 6).

In Figure 6 lines 1*A*, *AB*, *AC* are perpendicular to the corresponding sides of the triangles 2-3,1-2, 3-1. The angles of rotation of the sides are denoted respectively – $\varphi_{12}, \varphi_{23}, \varphi_{31}$. The values of angles of sides rotation can be easily determined by means of geometric scheme (Figure 6):

$$\varphi_{23} = \frac{1}{h_{23}}, \varphi_{12} = \frac{BB/}{AB} = \frac{\cos\beta_{31}}{h_{23}}, \varphi_{31} = \frac{CC/}{AC} = \frac{\cos\beta_{12}}{h_{23}}. \quad (41)$$

The moments M^n normal to the side of the element are directed oppositely with respect to internal moments and are expressed through the bending and twisting moments in the following form:

$$M_{ij}^n = -M_x \sin^2\alpha_{ij} - M_y \cos^2\alpha_{ij} + 2M_{xy}\sin\alpha_{ij}\cos\alpha_{ij}. \quad (42)$$

In (42) α_{ij} is the angle between the side $i-j$ of the element and the X axis.

$$\cos\alpha_{ij} = \frac{x_j - x_i}{l_{ij}}, \sin\alpha_{ij} = \frac{y_j - y_i}{l_{ij}}. \quad (43)$$

Using (42), (43), we obtain the expressions for the nodal moments directed perpendicular to the sides of the finite element (Figure 5):

$$\begin{aligned}
M_{1,1-2}^n &= -M_{x,1}\sin^2\alpha_{12} - M_{y,1}\cos^2\alpha_{12} + 2M_{xy,1}\sin\alpha_{12}\cos\alpha_{12},\\
M_{1,3-1}^n &= -M_{x,1}\sin^2\alpha_{31} - M_{y,1}\cos^2\alpha_{31} + 2M_{xy,1}\sin\alpha_{31}\cos\alpha_{31},\\
M_{2,1-2}^n &= -M_{x,2}\sin^2\alpha_{12} - M_{y,2}\cos^2\alpha_{12} + 2M_{xy,2}\sin\alpha_{12}\cos\alpha_{12},\\
M_{2,2-3}^n &= -M_{x,2}\sin^2\alpha_{23} - M_{y,2}\cos^2\alpha_{23} + 2M_{xy,2}\sin\alpha_{23}\cos\alpha_{23},\\
M_{3,2-3}^n &= -M_{x,3}\sin^2\alpha_{23} - M_{y,3}\cos^2\alpha_{23} + 2M_{xy,3}\sin\alpha_{23}\cos\alpha_{23},\\
M_{3,3-1}^n &= -M_{x,3}\sin^2\alpha_{31} - M_{y,3}\cos^2\alpha_{31} + 2M_{xy,3}\sin\alpha_{31}\cos\alpha_{31}.
\end{aligned} \quad (44)$$

Considering the piecewise constant approximation of the moments, the expression for the work of internal forces on possible displacement of node 1 (Figure 6) can be written in the following form:

$$\delta U_{1,z}^k = \frac{1}{2}M_{1,1-2}^n\varphi_{12}l_{12} + \frac{1}{2}M_{1,3-1}^n\varphi_{31}l_{31} + \frac{1}{2}M_{2,1-2}^n\varphi_{12}l_{12} - \frac{1}{2}M_{2,2-3}^n\varphi_{23}l_{23} - \frac{1}{2}M_{3,2-3}^n\varphi_{23}l_{23} + \frac{1}{2}M_{3,3-1}^n\varphi_{31}l_{31}. \quad (45)$$

Substituting (44) into (45), we obtain the expression for $\delta U_{1,z}^k$:

$$\begin{aligned}
\delta U_{1,z}^k = {} & \frac{M_{x,1}}{2h_{23}}(-l_{12}\sin^2\alpha_{12}\cos\beta_{31} - l_{31}\sin^2\alpha_{31}\cos\beta_{12}) +\\
& \frac{M_{y,1}}{2h_{23}}(-l_{12}\cos^2\alpha_{12}\cos\beta_{31} - l_{31}\cos^2\alpha_{31}\cos\beta_{12}) +\\
& \frac{M_{xy,1}}{2h_{23}}(2l_{12}\sin\alpha_{12}\cos\alpha_{12}\cos\beta_{31} + 2l_{31}\sin\alpha_{31}\cos\alpha_{31}\cos\beta_{12}) +\\
& \frac{M_{x,2}}{2h_{23}}(-l_{12}\sin^2\alpha_{12}\cos\beta_{31} + l_{23}\sin^2\alpha_{23}) +\\
& \frac{M_{y,2}}{2h_{23}}(-l_{12}\cos^2\alpha_{12}\cos\beta_{31} + l_{23}\cos^2\alpha_{23}) +\\
& \frac{M_{xy,2}}{2h_{23}}(2l_{12}\sin\alpha_{12}\cos\alpha_{12}\cos\beta_{31} - 2l_{23}\sin\alpha_{23}\cos\alpha_{23}) +\\
& \frac{M_{x,3}}{2h_{23}}(-l_{31}\sin^2\alpha_{31}\cos\beta_{12} + l_{23}\sin^2\alpha_{23}) +\\
& \frac{M_{y,3}}{2h_{23}}(-l_{31}\cos^2\alpha_{31}\cos\beta_{12} + l_{23}\cos^2\alpha_{23}) +\\
& \frac{M_{xy,3}}{2h_{23}}(2l_{31}\sin\alpha_{31}\cos\alpha_{31}\cos\beta_{12} - 2l_{23}\sin\alpha_{23}\cos\alpha_{23}).
\end{aligned} \quad (46)$$

To obtain the expression for the work of internal forces for possible displacement of node 2, we need to perform cyclic replacement of the indices in expression (46): replace index 1 by index 2, index 2 by 3, and index 3 replaced by index 1. Then we obtain the expression for $\delta U_{2,z}^k$:

$$\delta U_{2,z}^{k} = \frac{M_{x,2}}{2h_{31}}(-l_{23}\sin^2\alpha_{23}\cos\beta_{12} - l_{12}\sin^2\alpha_{12}\cos\beta_{23}) +$$
$$\frac{M_{y,2}}{2h_{31}}(-l_{23}\cos^2\alpha_{23}\cos\beta_{12} - l_{12}\cos^2\alpha_{12}\cos\beta_{23}) +$$
$$\frac{M_{xy,2}}{2h_{31}}(2l_{23}\sin\alpha_{23}\cos\alpha_{23}\cos\beta_{12} + 2l_{12}\sin\alpha_{12}\cos\alpha_{12}\cos\beta_{23}) +$$
$$\frac{M_{x,3}}{2h_{31}}(-l_{23}\sin^2\alpha_{23}\cos\beta_{12} + l_{31}\sin^2\alpha_{31}) +$$
$$\frac{M_{y,3}}{2h_{31}}(-l_{23}\cos^2\alpha_{23}\cos\beta_{12} + l_{31}\cos^2\alpha_{31}) + \quad (47)$$
$$\frac{M_{xy,3}}{2h_{31}}(2l_{23}\sin\alpha_{23}\cos\alpha_{23}\cos\beta_{12} - 2l_{31}\sin\alpha_{31}\cos\alpha_{31}) +$$
$$\frac{M_{x,1}}{2h_{31}}(-l_{12}\sin^2\alpha_{12}\cos\beta_{23} + l_{31}\sin^2\alpha_{31}) +$$
$$\frac{M_{y,1}}{2h_{31}}(-l_{12}\cos^2\alpha_{12}\cos\beta_{23} + l_{31}\cos^2\alpha_{31}) +$$
$$\frac{M_{xy,1}}{2h_{31}}(2l_{12}\sin\alpha_{12}\cos\alpha_{12}\cos\beta_{23} - 2l_{31}\sin\alpha_{31}\cos\alpha_{31}).$$

Performing the cyclic replacement of the indices again, we obtain an expression for $\delta U_{3,z}^{k}$:

$$\delta U_{3,z}^{k} = \frac{M_{x,3}}{2h_{12}}(-l_{31}\sin^2\alpha_{31}\cos\beta_{23} - l_{23}\sin^2\alpha_{23}\cos\beta_{31}) +$$
$$\frac{M_{y,3}}{2h_{12}}(-l_{31}\cos^2\alpha_{31}\cos\beta_{23} - l_{23}\cos^2\alpha_{23}\cos\beta_{31}) +$$
$$\frac{M_{xy,3}}{2h_{12}}(2l_{31}\sin\alpha_{31}\cos\alpha_{31}\cos\beta_{23} + 2l_{23}\sin\alpha_{23}\cos\alpha_{23}\cos\beta_{31}) +$$
$$\frac{M_{x,1}}{2h_{12}}(-l_{31}\sin^2\alpha_{31}\cos\beta_{21} + l_{12}\sin^2\alpha_{12}) +$$
$$\frac{M_{y,1}}{2h_{12}}(-l_{31}\cos^2\alpha_{31}\cos\beta_{23} + l_{12}\cos^2\alpha_{12}) + \quad (48)$$
$$\frac{M_{xy,1}}{2h_{12}}(2l_{31}\sin\alpha_{31}\cos\alpha_{31}\cos\beta_{23} - 2l_{12}\sin\alpha_{12}\cos\alpha_{12}) +$$
$$\frac{M_{x,2}}{2h_{12}}(-l_{23}\sin^2\alpha_{23}\cos\beta_{31} + l_{12}\sin^2\alpha_{12}) +$$
$$\frac{M_{y,2}}{2h_{12}}(-l_{23}\cos^2\alpha_{23}\cos\beta_{31} + l_{12}\cos^2\alpha_{12}) +$$
$$\frac{M_{xy,2}}{2h_{12}}(2l_{23}\sin\alpha_{23}\cos\alpha_{23}\cos\beta_{31} - 2l_{12}\sin\alpha_{12}\cos\alpha_{12}).$$

Let us unite the node moments in the global coordinate system XOY for the triangular finite element with the index k into the vector $\{M^k\}$.

$$\{M^k\}^T = (M_{x,1} \quad M_{y,1} \quad M_{xy,1} \quad M_{x,2} \quad M_{y,2} \quad M_{xy,2} \quad M_{x,3} \quad M_{y,3} \quad M_{xy,3}). \quad (49)$$

We also introduce vector combining the values of the work of internal forces for possible displacements of nodes of finite element:

$$\left\{\delta U_z^k\right\} = \begin{Bmatrix} \delta U_{1,z}^k \\ \delta U_{2,z}^k \\ \delta U_{3,z}^k \end{Bmatrix}. \quad (50)$$

Then we can write the matrix expression:

$$\{\delta U_z^k\} = [L^k]\{M^k\}. \quad (51)$$

The matrix $[L^k]$ has 3 rows and 9 columns. The elements of the matrix $[L^k]$ are coefficients under the corresponding moments in the expressions (46)–(48). From matrices $[L^k]$ for finite elements, in accordance with the numbering of nodes and elements, global "equilibrium" matrix $[L]$ is formed for the whole system.

The global equilibrium matrix $[L]$ for the whole system will have “tape-line” structure of non-zero elements. The number of rows of the matrix $[L]$ is equal to the number of unfixed nodes of the system n. Indexes for unknown moments are assigned in accordance with the numbering of nodes. Therefore, the width of the “tape” of non-zero elements of the matrix $[L]$ will be determined by the maximum difference of the node numbers of all finite elements adjoining to the node. For example, for node 13 in Figure 2 the maximum difference of the indexes of nodes, the finite elements adjoining it, $m_{p,13} = 18 - 7 = 11$. Accordingly, the width of the “tape” of non-zero elements for the row of the matrix $[L]$ corresponding to node 13, $m_{L,13} = (m_{p,13} + 1)3 = 36$. After calculating the width of the “tape” $m_{L,i}$ of the matrix $[L]$ for each of the rows, the maximum value $m_{L,max}$ is determined. Thus, for elements of the matrix $[L]$, we can use a rectangular array consisting of $m_{L,max}$ columns and n lines.

In addition, it is necessary to form an array Ind, consisting of two columns. In the first and second columns, respectively, the minimum and maximum indexes of finite element nodes, for each row of the matrix $[L]$, are stored. For example, for the row corresponding to node 13 in Figure 2, we obtain: $Ind[13,1] = 7, Ind[13,2] = 18$. The Ind array is used in the construction of the matrix multiplication algorithm for calculating the elements of the matrix $[K] = [L][D]^{-1}[L]^T$, and, also, for determining the width of the “tape” of non-zero elements of matrix $[K]$ – m_K.

The potential of external concentrated and evenly distributed loads for possible displacement of node i along the global coordinate axis is determined by formula (52).

$$\delta V_i = P_i + \frac{1}{3} q^k A^k = R_i. \quad (52)$$

P_i – the force concentrated at node i; q^k – uniformly distributed by element load. The generalized forces R_i are placed in the vector $\{F\}$ (see (12)).

3. Results and Discussion

According to the program developed in *MathCad 14.0*, calculations of square and rectangular plates were performed on the action of concentrated force and distributed load (Figure 7). Hinged-supported and clamped plates were calculated in accordance with the Kirchhoff theory. In the calculations, grids of rectangular and triangular finite elements were used. The plate has the following parameters: side length – $6m$ or $3m$, thickness – $1m$, modulus of elasticity $E = 10000\ kN/m^2$, Poisson's ratio $\mu = 0.3$, uniformly distributed load $q = 10\ kN/m^2$.

As consequence of the symmetry of the problem, the quarter of the plate was calculated, with the corresponding boundary conditions on the sides lying on the symmetry axes. At the nodes lying on the axes of symmetry, the torques were assumed to be zero. The bending moments directed along the plate boundary and moments directed perpendicular to the boundary were assumed to be zero in the support nodes of the hinged plates.

In [23] analytical solutions of the plate bending problems for various types of the support of sides for distributed and concentrated loads are presented. The displacements are expressed in the form:

$w = \alpha\frac{qa^4}{D}, w = \alpha\frac{Pa^2}{D}$, and moments in the form: $M = \beta qa^2, M = \beta P$. The coefficients for the variants of the calculation schemes are given in Table 1. $D = \frac{Et^3}{12(1-\mu^2)}$ - bending stiffness of a plate.

Table 1. Coefficients from [23] for the determination of analytical values

Sizes of sides	Support	Load	w_1 α	M_{y1} β	M_{x1} β	M_3 β	M_2 β
$a = b$	hinged	q	0.00406	0.0479	0.0479	-	-
$a = b$	clamped	q	0.00126	0.0231	0.0231	-0.0513	-0.0513
$a = b$	clamped	P	0.0056	-	-	-0.1257	-0.1257
$\frac{b}{a} = 2$	clamped	q	0.00254	0.0412	0.0158	-0.0571	-0.0829

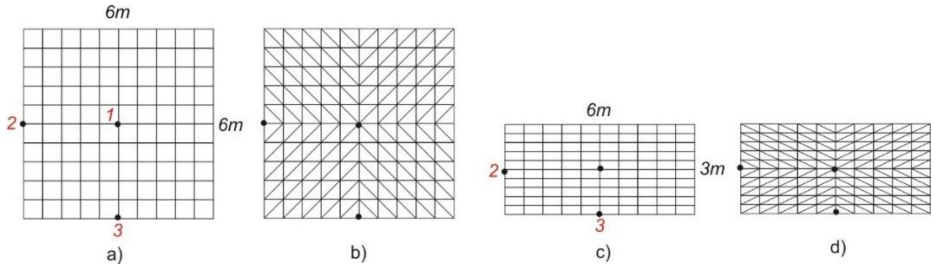

Figure 7. Finite element grids for square and rectangular plates: a) 5x5 square grid of finite elements; b) 5x5 grid of isosceles triangular finite elements; c) grid of 5x5 rectangular finite elements; d) grid of 5x5 elongated triangular finite elements

The results of calculations of plates according to the proposed method were compared with the results obtained by the finite elements method in the LIRA-SAPR program and analytical solutions. A comparison of solutions is shown in Figures 8–15 and in Tables 2–16. In the figures, the green line shows the analytical solutions from [23]. In the tables and in the figures, the grid parameters are indicated for the whole plate.

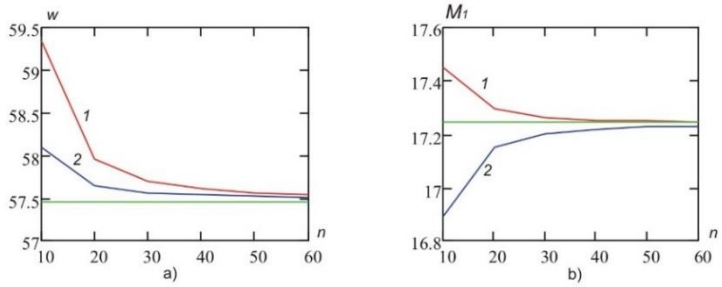

Figure 8. Hinged-supported square plate - rectangular finite elements (Figure 7a), $q = 10\ kN/m^2$: a) displacement of the center of the plate - *w*; b) the bending moment at the center of the plate is M_1. 1 – the solution in stresses; 2 – the solution in displacements (LIRA-SAPR)

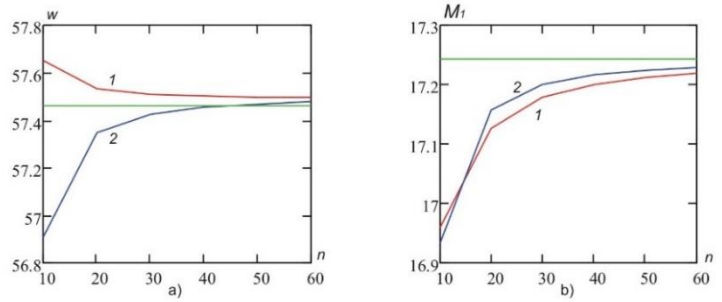

Figure 9. Hinged-supported square plate – triangular finite elements (Figure 7a), $q = 10\ kN/m^2$: a) displacement of the center of the plate – *w*; b) the bending moment at the center of the plate is M_1. 1 – the solution in stresses; 2 – the solution in displacements (LIRA-SAPR)

Table 2. The square plate with hinged supports, divided by the square finite elements (Figure 7a), $q = 10\ kN/m^2$.

Grid	Solution in stresses					Solution in displacements LIRA-SAPR			
	w, mm	M_1, *kNm/m*	$m_{L,max}$	m_K	*n*	*w, mm*	M_1, *kNm/m*	m_K	*n*
10x10	59.342	17.4523	41	15	25	58.097	16.8897	21	85
20x20	57.950	17.2919	71	25	100	57.643	17.1518	36	320
30x30	57.695	17.2625	101	35	225	57.559	17.2003	51	705
40x40	57.606	17.2523	131	45	400	57.530	17.2173	66	1240
50x50	57.565	17.2475	161	55	625	57.516	17.2251	81	1925
60x60	57.542	17.2449	191	65	900	57.509	17.2294	96	2760
Exact	57.458	17.244				57.458	17.244		
Error, %	0.15	0.005				0.09	0.08		

Table 3. The square plate with hinged supports, divided by the triangular finite elements (Figure 7b), $q = 10\ kN/m^2$.

Grid	Solution in stresses					Solution in displacements LIRA-SAPR			
	w, mm	M_1, *kNm/m*	$m_{L,max}$	m_K	*n*	*w, mm*	M_1, *kNm/m*	m_K	*n*
10x10	57.653	16.9602	41	15	25	56.910	16.9338	21	85
20x20	57.531	17.1260	71	25	100	57.348	17.1573	36	320
30x30	57.510	17.1777	101	35	225	57.423	17.2002	51	705
40x40	57.502	17.2002	131	45	400	57.456	17.2161	66	1240
50x50	57.499	17.2120	161	55	625	57.469	17.2238	81	1925
60x60	57.497	17.2191	191	65	900	57.476	17.2281	96	2760
Exact	57.458	17.244				57.458	17.244		
Error, %	0.07	0.14				0.03	0.09		

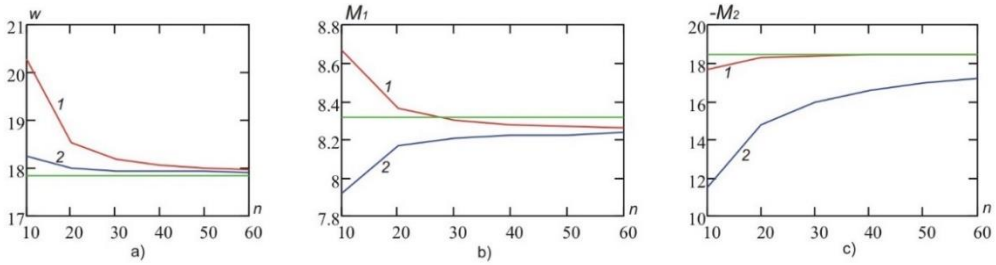

Figure 10. Clamped square plate - rectangular finite elements (Figure 7a), $q = 10\ kN/m^2$: a) displacement of the center of the plate – *w*; b) the bending moment at the center of the plate is M_1. c) the bending moment at the clamped side is M_2.1 – the solution in stresses; 2 – the solution in displacements (LIRA-SAPR)

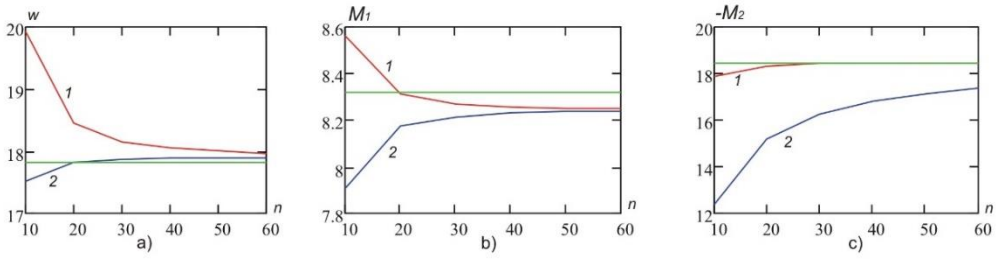

Tyukalov, Yu.Ya. Finite element models in stresses for bending plates. Magazine of Civil Engineering. 2018. 82(6). Pp. 170–190. doi: 10.18720/MCE.82.16

Figure 11. Clamped square plate - triangular finite elements (Figure 7b), $q = 10\ kN/m^2$: a) displacement of the center of the plate – *w*; b) the bending moment at the center of the plate is M_1. c) the bending moment at the clamped side is M_2. 1 – the solution in stresses; 2 – the solution in displacements (LIRA-SAPR)

Table 4. Clamped square plate - rectangular finite elements (Figure 7a), $q = 10\ kN/m^2$.

Grid	Solution in stresses			Solution in displacements LIRA-SAPR		
	w, mm	M_1, *kNm/m*	M_2, *kNm/m*	*w, mm*	M_1, *kNm/m*	M_2, *kNm/m*
10x10	20.293	8.66832	-17.65748	18.257	7.91934	-11.4736
20x20	18.537	8.36097	-18.25078	17.997	8.16432	-14.7482
30x30	18.193	8.29848	-18.37533	17.947	8.20962	-15.9398
40x40	18.069	8.27586	-18.42045	17.930	8.22546	-16.5550
50x50	18.012	8.26521	-18.44167	17.922	8.23280	-16.9304
60x60	17.980	8.25936	-18.45331	17.917	8.23678	-17.1833
Exact	17.832	8.316	-18.468	17.832	8.316	-18.468
Error, %	0.83	0.68	0.08	0.47	0.95	6.96

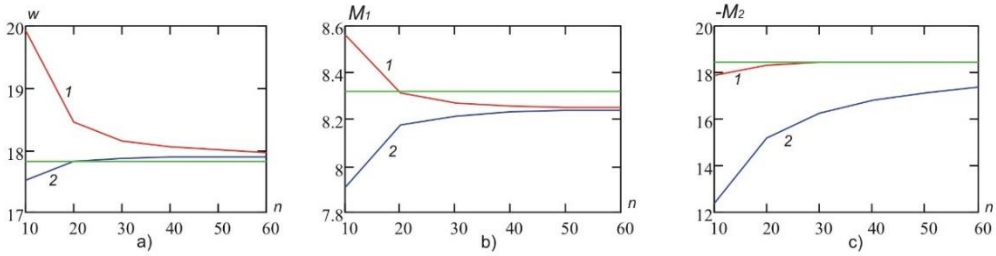

Figure 11. Clamped square plate - triangular finite elements (Figure 7b), $q = 10\ kN/m^2$: a) displacement of the center of the plate - *w*; b) the bending moment at the center of the plate is M_1. c) the bending moment at the clamped side is M_2. 1 - the solution in stresses; 2 - the solution in displacements (LIRA-SAPR).

Table 5. Clamped square plate - triangular finite elements (Figure 7b), $q = 10\ kN/m^2$.

Grid	Solution in stresses			Solution in displacements LIRA-SAPR		
	w, mm	M_1, *kNm/m*	M_2, *kNm/m*	*w, mm*	M_1, *kNm/m*	M_2, *kNm/m*
10x10	19.921	8.56379	-17.86275	17.251	7.90791	-12.3842
20x20	18.449	8.30952	-18.34177	17.826	8.17397	-15.2137
30x30	18.154	8.26870	-18.42369	17.875	8.21509	-16.2554
40x40	18.048	8.25636	-18.45019	17.890	8.22875	-16.7944
50x50	17.998	8.25136	-18.46175	17.897	8.23494	-17.1235
60x60	17.970	8.24898	-18.46776	17.900	8.23827	-17.3453
Exact	17.832	8.316	-18.468	17.832	8.316	-18.468
Error, %	0.77	0.81	0.001	0.38	0.93	6.08

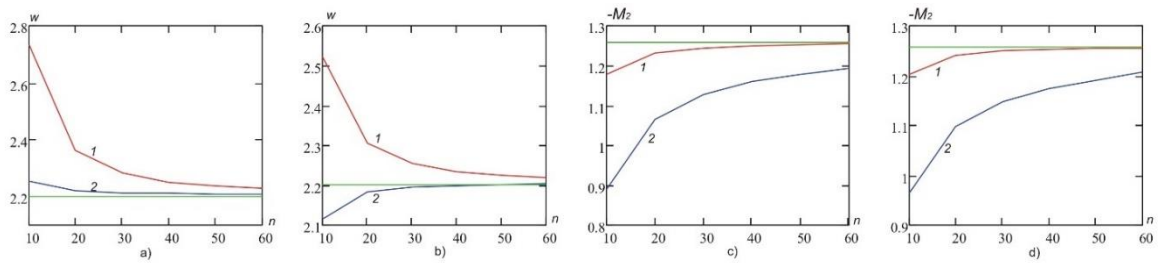

Figure 12. Clamped square plate - the action of concentrated force in the center $P = 10\ kN$: a) square finite elements – displacement of the center of the plate *w*; b) triangular finite elements - displacement of the center of the plate *w*; c) square finite elements - moments in clamped side M_2; d) triangular finite elements - moments in clamped side M_2. 1 – solution in stresses; 2 – solution in displacements LIRA-SAPR

Table 6. The clamped square plate. The action of the concentrated force $P = 10\ kN$.

Grid	Solution in stresses				Solution in displacements LIRA-SAPR			
	square elements		triangular elements		square elements		triangular elements	
	w, mm	M_2, *kNm/m*	*w, mm*	M_2, *kNm/m*	*w, mm*	M_2, *kNm/m*	*w, mm*	M_2, *kNm/m*
10x10	2.7351	-1.17795	2.5213	-1.20274	2.2548	-0.8901	2.1160	-0.96346
20x20	2.3638	-1.23115	2.3044	-1.24078	2.2115	-1.0659	2.1833	-1.09814
30x30	2.2826	-1.24479	2.2546	-1.24980	2.2138	-1.1262	2.1945	-1.14827
40x40	2.2517	-125012	2.2352	-1.25319	2.2108	-1.1604	2.1994	-1.17446
50x50	2.2365	-1.25273	2.2257	-1.25481	2.2093	-1.1792	2.2017	-1.19056
60x60	2.2279	-1.25420	2.2202	-1.25569	2.2084	-1.1922	2.2030	-1.20686
Exact	2.2015	-1.257	2.2015	-1.257	2.2015	-1.257	2.2015	-1.257
Error, %	1.1	0.22	0.85	0.1	0.31	5.16	0.07	3.99

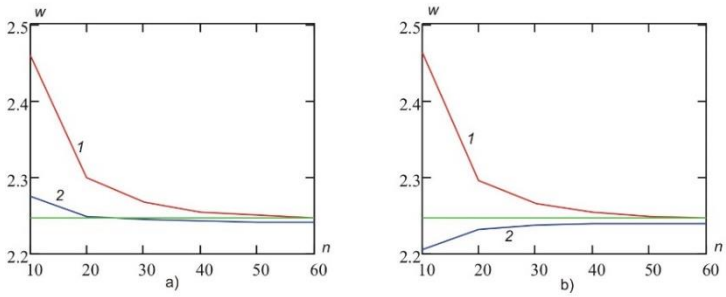

Figure 13. The displacements of the center of rectangular clamped plate (Figure 7c, 7d) under the action of load $q = 10\ kN/m^2$: a) rectangular finite elements; b) triangular finite elements. 1 – solution in stresses; 2 – solution in displacements LIRA-SAPR

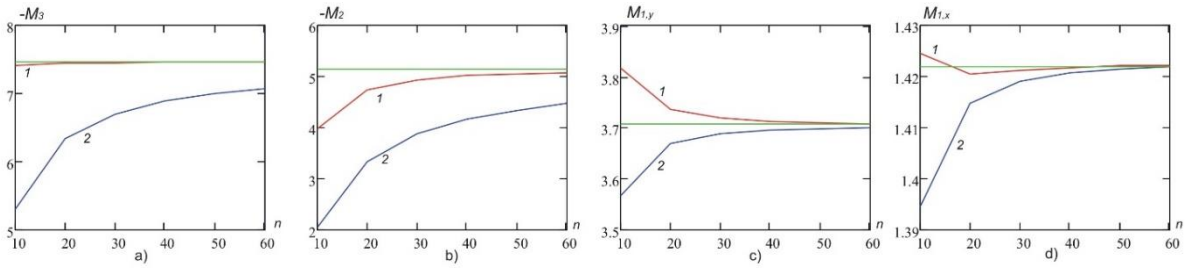

Figure 14. Bending moments in rectangular clamped plate under the action of load $q = 10\ kN/m^2$ for rectangular grid of finite elements (Figure 7c)

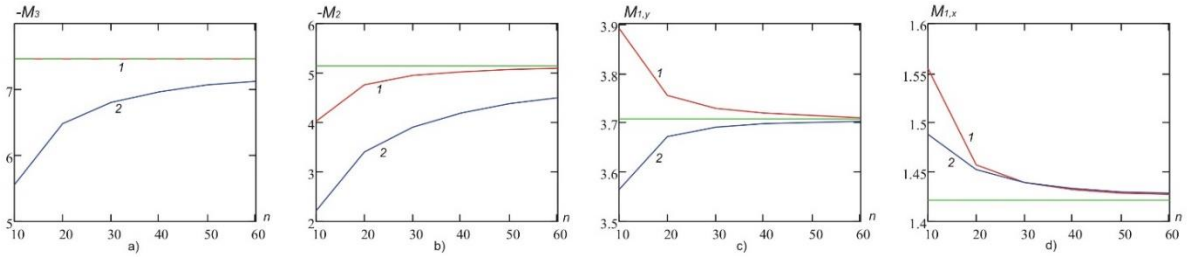

Figure 15. Bending moments in rectangular clamped plate under the action of load $q = 10\ kN/m^2$ for triangular grid of finite elements (Figure 7d)

Tyukalov, Yu.Ya. Finite element models in stresses for bending plates. Magazine of Civil Engineering. 2018. 82(6). Pp. 170–190. doi: 10.18720/MCE.82.16

Table 7. The clamped rectangular plate (Figure 7c) – rectangular finite elements. Load action $q = 10\ kH/m^2$

Grid	Solution in stresses					Solution in displacements LIRA-SAPR				
	w, mm	M_3, kNm/m	M_2, kNm/m	M_{y1}, kNm/m	M_{x1}, kNm/m	*w, mm*	M_3, kNm/m	M_2, kNm/m	M_{y1}, kNm/m	M_{x1}, kNm/m
10x10	2.4658	-7.41651	-3.97326	3.81770	1.42455	2.2747	-5.30885	-2.04139	3.56671	1.39448
20x20	2.2990	-7.45081	-4.73785	3.73492	1.42046	2.2491	-6.34108	-3.33420	3.66967	1.41457
30x30	2.2668	-7.45332	-4.93844	3.71812	1.42127	2.2443	-6.70369	-3.87049	3.68882	1.41906
40x40	2.2554	-7.45663	-5.01715	3.71203	1.42178	2.2426	-6.88858	-4.16096	3.69544	1.42065
50x50	2.2500	-7.45716	-5.05563	3.70917	1.42207	2.2418	-7.00068	-4.34272	3.69850	1.42139
60x60	2.2471	-7.45743	-5.07722	3.70759	1.42225	2.2414	-7.07590	-4.46709	3.70017	1.42180
Exact	2.2467	-7.461	-5.139	3.708	1.422	2.2467	-7.461	-5.139	3.708	1.422
Error, %	0.02	0.05	1.2	0.01	0.02	0.24	5.16	13.07	0.2	0.01

Table 8. The clamped rectangular plate (Figure 7d) – triangular finite elements. Load action $\boldsymbol{q = 10\ kH/m^2}$

Grid	Solution in stresses					Solution in displacements LIRA-SAPR				
	w, mm	M_3, kNm/m	M_2, kNm/m	M_{y1}, kNm/m	M_{x1}, kNm/m	*w, mm*	M_3, kNm/m	M_2, kNm/m	M_{y1}, kNm/m	M_{x1}, kNm/m
10x10	2.46209	-7.47306	-4.0175	3.88984	1.55522	2.20474	-5.55454	-2.21824	3.56493	1.48789
20x20	2.29638	-7.46733	-4.7710	3.75561	1.45769	2.23251	-6.48844	-3.39414	3.67033	1.45181
30x30	2.26548	-7.46316	-4.9588	3.72829	1.43891	2.23718	-6.80927	-3.91612	3.69106	1.43924
40x40	2.25459	-7.46118	-5.0306	3.71818	1.43215	2.23871	-6.97098	-4.20201	3.69753	1.43348
50x50	2.24952	-7.46013	-5.0652	3.71332	1.42894	2.23938	-7.06830	-4.38058	3.70025	1.43034
60x60	2.24676	-7.45951	-5.0843	3.71060	1.42714	2.23973	-7.13339	-4.50216	3.70160	1.42843
Exact	2.2467	-7.461	-5.139	3.708	1.422	2.2467	-7.461	-5.139	3.708	1.422
Error, %	0.0003	0.02	1.06	0.07	0.14	0.3	4.39	12.4	0.17	0.45

Table 9. Errors in calculating bending moments, expressed in percent

Grid	Support	Load	Solution in stresses				Solution in displacements LIRA-SAPR			
			M_3	M_2	M_{y1}	M_{x1}	M_3	M_2	M_{y1}	M_{x1}
Figure 7a	hinged	*q*	-	-	0.005	0,005	-	-	0,08	0,08
Figure 7b	hinged	*q*	-	-	0.14	0.14	-	-	0.09	0.09
Figure 7a	clamped	*q*	0.08	0.08	0.68	0.68	6.96	6.96	0.95	0.95
Figure 7b	clamped	*q*	0.001	0.001	0.81	0.81	6.08	6.08	0.93	0.93
Figure 7a	clamped	*P*	0.22	0.22	-	-	5.16	5.16	-	-
Figure 7b	clamped	*P*	0.1	0.1	-	-	3.99	3.99	-	-
Figure 7c	clamped	*q*	0.05	1.2	0.01	0.02	5.16	13.07	0.2	0.01
Figure 7d	clamped	*q*	0.02	1.06	0.07	0.14	4.39	12.4	0.17	0.45

By beginning we estimate the convergence of displacements determined by the proposed calculation method in stresses and by the finite element method in displacements:

- for all the considered variants of calculation schemes and loads, the displacements obtained in the stresses, when crushing the grid, tend to the exact values from above - the proposed solution is more flexible and has the property of convergence of displacements from above;
- the solution in displacements (LIRA-SAPR) tends to the exact value from above if rectangular elements are used, and from below, if triangular elements are used - in one case the solution is more flexible, in the other case it is more rigid.

Analysis of the obtained results allows us to do the following conclusions about the accuracy of calculating bending moments (Table 9):

- the proposed solution method in stresses makes it possible to obtain the values of the bending moments with greater accuracy than the finite element method in displacements (LIRA-SAPR) for all the considered plate bending problems;
- the greatest error in calculating the moments for solving in stresses is 0.8 %, and for the finite element method in displacements (LIRA-SAPR), the error in calculating the moments in the clamped sides reaches 13 %;
- when using elongated rectangular and triangular elements (Figure 7c, d), the accuracy of calculating the bending moments according to the proposed technique in stresses is reduced a little;
- when calculating by the finite element method in displacements (LIRA-SAPR), the moments are determined for the centers of the finite elements, but for calculation in stresses – for the finite elements nodes;

It is also necessary to note the following computational features of obtaining the solution in stresses:

- additional computational costs associated with matrix multiplication $[L][D]^{-1}[L]^T$ are necessary to form the resolving system of linear equations. Since the matrix $[D]^{-1}$ is block-diagonal (block size 3x3), and the matrix $[L]$ has form of tape (the width of the tape of non-zero elements $m_{L,max}$ of Tables 2–3), we can use the special algorithm of multiplication of matrices, allowing to reduce computational costs;
- the resolving system of linear equations, in comparison with the solution by the finite element method in displacements, has a smaller number of unknowns n and a smaller width of the tape of non-zero elements m_K (Tables 2–3).

The paper [29] compares the results of calculations of clamped plates on the action of a uniformly distributed load for four types of triangular finite elements: BZIC is uncoordinated element of the displacement method [24, 30, 31]; TEC is element with forced compatibility of the inclination angles of the normal [26]; DKT is discrete Kirchhoff theory triangular element [30–31]; HSM is triangular hybrid finite element [33]. In Tables 10–11, the results of calculations for clamped square and rectangular plates, with a ratio of sides of 2 to 1, obtained for action uniformly distributed load, are compared. In Tables 10–11 shows the results of calculations for finite element grid 11 x 11 (for quarter of a plate), which corresponds to an 22 x 22 grid for the whole plate. In the tables, the solutions obtained by the proposed finite element method in stresses is designated FEM-S.

Table 10. A clamped square plate under the action of a uniformly distributed load. A grid of 11x11 for a quarter of the plate

Type of element	wD/qa^4	Error, %	M_1/qa^2	Error, %	M_2/qa^2	Error, %
BZIC	0,001277	+1.3	0,02374	+2.8	-0,05522	+7.6
TEC	0,001269	+0.7	0,02673	+15.7	0,05455	+6.3
DKT	0.001279	+1.5	0.02331	+0.91	-0.05212	+1.6
HSM	0.001269	+0.7	0.02325	+0.65	-0.05068	-1.2
FEM-S	0.001297	+2.9	0.023045	-0.24	-0.05102	-0.55
Exact	0.00126		0.0231		-0.0513	

Table 11. A clamped rectangular plate (b / a = 2) under the action of a uniformly distributed load. A grid of 11x11 for a quarter of the plate

Type of element	wD/qa^4	Error, %	$M_{1,x}/qa^2$	Error, %	$M_{1,y}/qa^2$	Error, %
BZIC	0.002583	+1.7	0.04216	+2.33	0.01495	-5.4
TEC	0.002551	+0.4	0.04666	+13.2	0.01888	+19.5
DKT	0.002566	+1.0	0.04188	+1.65	0.01650	+4.4
HSM	0.002541	0	0.04193	+1.77	0.01697	+7.4
FEM-S	0.002585	+1.8	0.041636	+1.06	0.016132	+2.1
Exact	0.00254		0.0412		0.0158	

Comparison of the values in Tables 10-11 allows us to have the following conclusions:

- rate of convergence of displacements obtained by the proposed method at stresses lower than the rate of convergence of displacements for finite elements TEC, DKT, HSM; for elongated finite elements rate of convergence of displacements, obtained by method in stresses, is near to the rate of convergence of displacements for the BZIC element (Table 11);
- the rate of convergence of the bending moments obtained by the proposed method in the stresses is higher than the rate of convergence of the moments obtained by the method with other considered finite elements;
- the use of elongated finite elements (Table 11) to a lesser degree leads to an increase in the error in calculating the moments by the proposed solution method in stresses, then for other considered finite elements; especially, this applies to bending moments in clamped sides of plate.

Note, that in constructing solution by the proposed technique in stresses, unlike traditional finite element method, we do not form stiffness matrix or flexible matrix for the finite element. A matrix of coefficients of system of linear algebraic equations for the whole system is directly formed. This matrix can be considered a stiffness matrix of the system, since it connects the displacements of nodes with external forces. When constructing the solutions by the proposed method, there is no need to apply any approximating functions for displacements at the finite element domain. For the solution, only approximations of the fields of possible displacements are used, which can be arbitrary, satisfying the kinematic boundary conditions. This approach is general and is applicable to solving various problems of building mechanics: flat and volume problems of the theory of elasticity, shell calculations, calculation of rod systems [20, 21].

4. Conclusion

1. The presented method of calculating the bent plates according to the Kirchhoff theory by the finite element method in stresses has property of convergence from above – the displacements obtained by this method converge to the exact values from above.

2. The solution by method in stresses requires large computational costs when obtaining elements of matrix of the resolving system of linear algebraic equations, but the number of unknowns and the width of the tape of non-zero elements is less than when solving by the finite element method in displacements.

3. When solving by method in stresses, the values of moments is determined directly at nodes of finite element grid, and not at the centers of the finite elements, which allows obtaining more accurate values of the moments, especially in the clamped nodes.

4. The proposed method of solving in stresses is based on the fundamental principles of structural mechanics – the principle of minimum of additional energy and the principle of possible displacements. Constant functions are used to approximate the forces, and linear ones are used for possible displacements, which ensures the convergence of the approximate solution to the exact solution, when we crush the finite element grid.

References

1. Zenkevich, O. Metod konechnykh elementov v tekhnike [Finite element method in engineering]. Moscow: Mir, 1975. 541 p. (rus)
2. Gallager, R. Metod konechnykh elementov. Osnovy [Finite element method. Basics]. Moskow: Mir, 1984. 428 p. (rus)
3. Karttunen, A.T., von Hertzen, R., Reddy, J.N., Romanoff, J. Exact elasticity-based finite element for circular plates. Computers & Structures. 2017. Vol. 182. Pp. 219–226.
4. Nguyen-Xuan, H. A polygonal finite element method for plate analysis. Computers & Structures. 2017. Vol. 188. Pp. 45–62.
5. Karttunen, A.T., von Hertzen, R., Reddy, J.N., Romanoff, J. Shear deformable plate elements based on exact elasticity solution. Computers & Structures. 2018. Vol. 200. Pp. 21–31.
6. Fallah N. On the use of shape functions in the cell centered finite volume formulation for plate bending analysis based on Mindlin-Reissner plate theory. Computers & Structures. 2006. Vol. 84. Pp. 1664–1672.
7. Klochkov, Yu.V., Vakhnina, O.V., Kiseleva, T.A. Raschet tonkikh obolochek na osnove treugolnogo konechnogo

Литература

1. Зенкевич О. Метод конечных элементов в технике. М.: Мир, 1975. 541 с.
2. Галлагер Р. Метод конечных элементов. Основы. М.: Мир, 1984. 428 с.
3. Karttunen A.T., von Hertzen R., Reddy J.N., Romanoff J. Exact elasticity–based finite element for circular plates // Computers & Structures. 2017. Vol. 182. Pp. 219–226.
4. Nguyen-Xuan H. A polygonal finite element method for plate analysis // Computers & Structures. 2017. Vol. 188. Pp. 45–62.
5. Karttunen A.T., von Hertzen R., Reddy J.N., Romanoff J. Shear deformable plate elements based on exact elasticity solution // Computers & Structures. 2018. Vol. 200. Pp. 21–31.
6. Fallah N. On the use of shape functions in the cell centered finite volume formulation for plate bending analysis based on Mindlin–Reissner plate theory // Computers & Structures. 2006. Vol. 84. Pp. 1664–1672.
7. Клочков Ю.В., Вахнина О.В., Киселева Т.А. Расчет тонких оболочек на основе треугольного конечного элемента с корректирующими множителями Лагранжа //

Тюкалов Ю.Ю. Конечно элементные модели в напряжениях для изгибаемых пластин // Инженерно-строительный журнал. 2018. № 6(82). С. 170–190.

elementa s korrektiruyushchimi mnozhitelyami Lagranzha [Calculation of thin shells on the basis of a triangular finite element with correcting Lagrange multipliers]. Stroitelnaya mekhanika inzhenernykh konstruktsiy i sooruzheniy. 2015. No. 5. Pp. 55–59. (rus)

8. Serpik, I.N. Development of a new finite element for plate and shell analysis by application of generalized approach to patch test. Fin. Elem. Anal. Design. 2010. Vol. 46. Pp. 1017–1030.
9. Zhang D.-G. Non-linear bending analysis of super elliptical thin plates. International Journal of Non-Linear Mechanics. 2013. Vol. 55. Pp. 180–185.
10. Mileykovskiy I.Ye., Traynin L.A. Effektivnyye izoparametricheskiye elementy plastin sredney tolshchiny [Effective isoparametric elements of plates of medium thickness]. Stroitelnaya mekhanika i raschet sooruzheniy. 1982. No. 5. Pp. 10–14. (rus)
11. Asemi, K., Salehi, M., Akhlaghi, M. Post-buckling analysis of FGM annular sector plates based on three dimensional elasticity graded finite elements. International Journal of Non-Linear Mechanics. 2014. Vol. 67. Pp. 164–177.
12. Rodrigues, J.D., Natarajan, S., Ferreira, A.J.M., Carrera, E., Bordas, S.P.A. Analysis of composite plates through cell–based smoothed finite element and 4-noded mixed interpolation of tensorial components techniques. Computers & Structures. 2014. Vol. 135. Pp. 83–87.
13. Ignatyev, A.V., Yefremova, N.S. Raschet kosougolnoy plastiny po metodu konechnykh elementov v forme klassicheskogo smeshannogo metoda [Calculation of an oblique plate by the finite element method in the form of a classical mixed method]. Stroitelnaya mekhanika i konstruktsii. 2016. No. 12. Pp. 39–44. (rus)
14. Kulikov, G., Plotnikova, S. A hybrid–mixed four–node quadrilateral plate element based on sampling surfaces method for 3D stress analysis. International journal for numerical methods in engineering. 2016. Vol. 108. No. 1. Pp. 26–54.
15. Mu, L., Wang, J., Ye, X. A hybridized formulation for the weak Galerkin mixed finite element method. Journal of Computational and Applied Mathematics. 2016. Vol. 307. Pp. 335–345.
16. Sukhoterin, M.V., Baryshnikov, S.O., Knysh, T.P. Stress–strain state of clamped rectangular Reissner plates. Magazine of Civil Engineering. 2017. No. 8(76). Pp. 225–240.
17. Tyukalov, Yu.Ya. Variatsionno–setochnyy metod resheniya zadach izgiba plit v napryazheniyakh [Variational–grid method for solving plate bending problems in stresses]. Izvestiya vysshikh uchebnykh zavedeniy. Stroitelstvo. 2006. No. 8. Pp. 13–20. (rus)
18. Tyukalov, Yu.Ya. Raschet plit na dinamicheskiye vozdeystviya s uchetom plasticheskikh deformatsiy [Calculation of plates for dynamic effects with allowance for plastic deformations]. Seysmostoykoye stroitelstvo. Bezopasnost sooruzheniy. 2005. No. 2. Pp. 24–26. (rus)
19. Tyukalov, Yu.Ya. Raschet obolochek proizvolnoy formy metodom konechnykh elementov v napryazheniyakh [Calculation of shells of arbitrary shape by the finite element method in stresses]. Stroitelnaya mekhanika i raschet sooruzheniy. 2006. No. 1. Pp. 65–74. (rus)
20. Tyukalov, Yu.Ya. The functional of additional energy for stability analysis of spatial rod systems. Magazine of Civil Engineering. 2017. No. 2(70). Pp. 18–32.
21. Tyukalov, Yu.Ya. Finite element models in stresses for plane elasticity problems. Magazine of Civil Engineering. 2018. No. 1(77). Pp. 23–37.
22. Sekulovich, M. Metod konechnykh elementov [Finite Element Method]. Moskow: Stroyizdat, 1993. 664 p. (rus)

Строительная механика инженерных конструкций и сооружений. 2015. № 5. С. 55–59.

8. Serpik I.N. Development of a new finite element for plate and shell analysis by application of generalized approach to patch test // Fin. Elem. Anal. Design. 2010. Vol. 46. Pp. 1017–1030.
9. Zhang D.-G.. Non-linear bending analysis of super elliptical thin plates // International Journal of Non-Linear Mechanics. 2013. Vol. 55. Pp. 180–185.
10. Милейковский И.Е., Трайнин Л.А. Эффективные изопараметрические элементы пластин средней толщины // Строительная механика и расчёт сооружений.1982. № 5. С. 10–14.
11. Asemi K., Salehi M., Akhlaghi M. Post-buckling analysis of FGM annular sector plates based on three dimensional elasticity graded finite elements // International Journal of Non-Linear Mechanics. 2014. Vol. 67. Pp. 164–177.
12. Rodrigues J.D., Natarajan S., Ferreira A.J.M., Carrera E., Bordas S.P.A. Analysis of composite plates through cell–based smoothed finite element and 4-noded mixed interpolation of tensorial components techniques // Computers & Structures. 2014. Vol. 135. Pp. 83–87.
13. Игнатьев А.В., Ефремова Н.С. Расчёт косоугольной пластины по методу конечных элементов в форме классического смешанного метода // Строительная механика и конструкции. 2016. № 12. С. 39–44.
14. Kulikov G., Plotnikova S. A hybrid-mixed four-node quadrilateral plate element based on sampling surfaces method for 3D stress analysis // International journal for numerical methods in engineering. 2016. Vol. 108. № 1. Pp. 26–54.
15. Mu L., Wang J., Ye X. A hybridized formulation for the weak Galerkin mixed finite element method // Journal of Computational and Applied Mathematics. 2016. Vol. 307. Pp. 335–345.
16. Сухотерин М.В., Барышников С.О., Кныш Т.П. Напряженно-деформированное состояние защемленной прямоугольной пластины Рейсснера // Инженерно-строительный журнал. 2017. № 8(76). С. 225–240.
17. Тюкалов Ю.Я. Вариационно-сеточный метод решения задач изгиба плит в напряжениях // Известия высших учебных заведений. Строительство. 2006. № 8. С. 13– 20.
18. Тюкалов Ю.Я. Расчет плит на динамические воздействия с учетом пластических деформаций // Сейсмостойкое строительство. Безопасность сооружений. 2005. № 2. С. 24–26.
19. Тюкалов Ю.Я. Расчет оболочек произвольной формы методом конечных элементов в напряжениях // Строительная механика и расчет сооружений. 2006. № 1. С. 65–74.
20. Тюкалов Ю.Я. Функционал дополнительной энергии для анализа устойчивости пространственных стержневых систем // Инженерно-строительный журнал. 2017. № 2(70). С. 18–32.
21. Тюкалов Ю.Я. Конечно элементные модели в напряжениях для задач плоской теории упругости // Инженерно-строительный журнал. 2018. № 1(77). С. 23–37.
22. Секулович М. Метод конечных элементов. М.: Стройиздат, 1993. 664 с.
23. Тимошенко С.П., Войновский–Кригер С. Пластины и оболочки. М.: Наука, 1966. 636 с.
24. Cheung Y.K., Chen W.J. Refined nine–parameter triangular thin plate bending element by using refined direct stiffness method // Int. J. for Num. Meth. In Eng. 1995. Vol. 38. Pp. 283–298.

Tyukalov, Yu.Ya. Finite element models in stresses for bending plates. Magazine of Civil Engineering. 2018. 82(6). Pp. 170–190. doi: 10.18720/MCE.82.16

23. Timoshenko, S.P., Voynovskiy–Kriger, S. Plastiny i obolochki [Plates and Shells]. Moskow: Nauka, 1966. 636 p. (rus)
24. Cheung, Y.K., Chen, W.J. Refined nine–parameter triangular thin plate bending element by using refined direct stiffness method // Int. J. for Num. Meth. In Eng. 1995. Vol. 38. Pp. 283–298.
25. Allman, D.J. A simple cubic displacement element for plate bending // Int. J. Numer. Meth. Eng. 1976. Vol. 10. No. 2. Pp. 263–281.
26. Kharvi, D., Kilsi, S. Izgibnyye elementy v vide treugolnykh plastinok s prinuditelnoy sovmestnostyu [Flexural elements in the form of triangular plates with forced compatibility]. Raketnaya tekhnika i kosmonavtika. 1971. Vol. 9. No. 6. Pp. 38–42. (rus)
27. Pian, T.H.H., Tong, P. Basis of finite methods for solid continua // Int. J. Numer. Meth. Eng. 1969. Vol. 1. Pp. 3–28.
28. Tong, P. New displacement hybrid finite element for solid continua // Int. J. Numer. Meth. Eng. 1970. Vol. 2. Pp. 3–28.
29. Belkin, A.Ye., Gavryushin, S.S. Raschet plastin metodom konechnykh elementov [Calculation of plates by the finite element method]. Moskow: MGTU, 2008. 231 p. (rus)
30. Batoz, J.L., Bathe, K.J., Ho, L.W. A study of three–node triangular plate bending elements // Int. J. Num. Meth. In Eng. 1980. Vol. 15. Pp. 1771–1812.
31. Batoz, J.L., Ben Tahor, M. Evaluation of a new quadrilateral thin plate bending element // Int. J. Num. Meth. Eng. 1982. Vol. 18. Pp. 1665–1677.
32. Haugender, E. A new penalty function element for thin shell analysis // Int. J. Num. Meth. in Eng. 1982. Vol. 18. Pp. 845–861.
33. Fraeijs de Veubeke, B., Sander, G. An equilibrium model for plate bending // Int. J. Solids and Str. 1968. Vol. 4. Pp. 447–468.
34. Bucalem, M.L., Bathe, K.J. Higher-order MITC general shell elements // Int. J. Num. Meth. In Eng. 1993. Vol. 36. Pp. 3729–3754.
35. Lee, S.W., Zhang, J. C. A six-node finite element for plate bending // Int. J. Num. Meth. In Eng. 1985. Vol. 21. Pp. 131–143.

25. Allman D.J. A simple cubic displacement element for plate bending // Int. J. Numer. Meth. Eng. 1976. Vol. 10. No. 2. Pp. 263–281.
26. Харви Д., Килси С. Изгибные элементы в виде треугольных пластинок с принудительной совместностью // Ракетная техника и космонавтика. 1971. Т. 9ю № 6. С. 38–42.
27. Pian T.H.H., Tong P. Basis of finite methods for solid continua // Int. J. Numer. Meth. Eng. 1969. Vol. 1. Pp. 3–28.
28. Tong P. New displacement hybrid finite element for solid continua // Int. J. Numer. Meth. Eng. 1970. Vol. 2. Pp. 3–28.
29. Белкин А.Е., Гаврюшин С.С. Расчет пластин методом конечных элементов. М.: МГТУ, 2008. 231 с.
30. Batoz J.L., Bathe K.J., Ho L.W. A study of three–node triangular plate bending elements // Int. J. Num. Meth. In Eng. 1980. Vol. 15. Pp. 1771–1812.
31. Batoz J.L., Ben Tahor M. Evaluation of a new quadrilateral thin plate bending element // Int. J. Num. Meth. Eng. 1982. Vol. 18. Pp. 1665–1677.
32. Haugender E. A new penalty function element for thin shell analysis // Int. J. Num. Meth. in Eng. 1982. Vol. 18. Pp. 845–861.
33. Fraeijs de Veubeke B., Sander G. An equilibrium model for plate bending // Int. J. Solids and Str. 1968. Vol. 4. Pp. 447–468.
34. Bucalem M.L., Bathe K.J. Higher-order MITC general shell elements // Int. J. Num. Meth. In Eng. 1993. Vol. 36. Pp. 3729–3754.
35. Lee S.W., Zhang J. C. A six-node finite element for plate bending // Int. J. Num. Meth. In Eng. 1985. Vol. 21. Pp. 131–143.

Yury Tyukalov,
+7(912)8218977; yutvgu@mail.ru

Юрий Яковлевич Тюкалов,
+7(912)8218977; эл. почта: yutvgu@mail.ru

Тюкалов Ю.Ю. Конечно элементные модели в напряжениях для изгибаемых пластин // Инженерно-строительный журнал. 2018. № 6(82). С. 170–190.